CONF-9505264--24

UCRL-JC-120220
PREPRINT

Thermal Management in Inertial Fusion Energy Slab Amplifiers

S. B. Sutton
G. F. Albrecht

This paper was prepared for submittal to the
1st Annual International Conference on Lasers for
Application to Inertial Confinement Fusion
Monterey, CA
May 30 - June 2, 1995

July 17, 1995

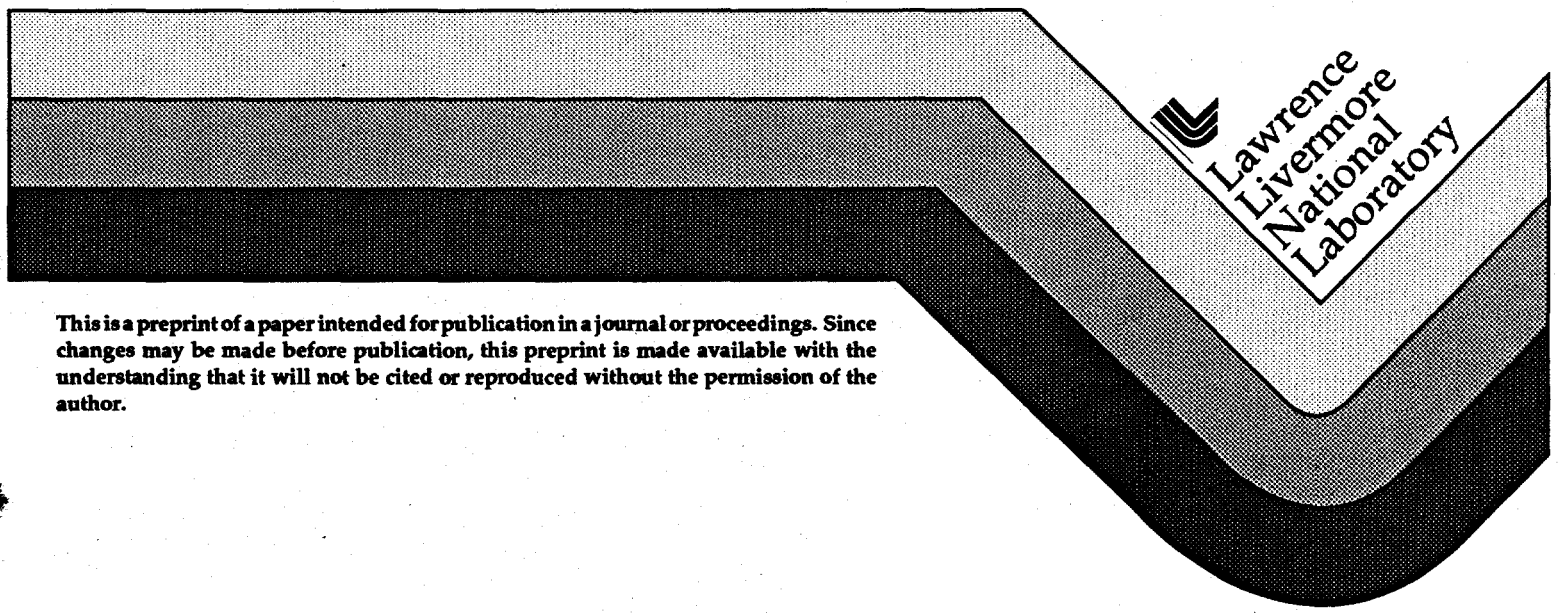

DISCLAIMER

Portions of this document may be illegible in electronic image products. Images are produced from the best available original document.

Thermal Management in Inertial Fusion Energy Slab Amplifiers

Steven B. Sutton and Georg F. Albrecht

Lawrence Livermore National Laboratory
P.O. Box 808, L-495
Livermore, CA 94550

ABSTRACT

As the technology associated with the development of solid-state drivers for inertial fusion energy (IFE) has evolved, increased emphasis has been placed on the development of an efficient approach for managing the waste heat generated in the laser media. This paper addresses the technical issues associated with the gas cooling of large aperture slabs, where the laser beam propagates through the cooling fluid. It is shown that the major consequence of proper thermal management is the introduction of simple wedge, or beam steering, into the system.

Achieving proper thermal management requires careful consideration of the geometry, cooling fluid characteristics, cooling flow characteristics, as well as the thermal/mechanical/optical characteristics of the laser media. Particularly important are the effects of cooling rate variation and turbulent scattering on the system optical performance. Helium is shown to have an overwhelming advantage with respect to turbulent scattering losses. To mitigate cooling rate variations, we introduce the concept of flow conditioning. Finally, optical path length variations across the aperture are calculated. A comparison of two laser materials (S-FAP and YAG) shows the benefit of a nearly a-thermal material on optical variations in the system.

Keywords: slab amplifier, inertial fusion energy, optical distortion, convective heat transfer, turbulent scattering, gas cooling

1. INTRODUCTION

Over the past decade, significant advancements have been made in the development of advanced laser materials and efficient, long-life, high-power semi-conductor diodes.[1,2] With these improvements, there has been renewed interest in the development of a practical concept for a diode pumped solid-state inertial fusion energy (IFE) driver.[3] Since the thermal load on the solid-state laser medium can be nearly as much as the output power from the laser, efficient removal of the waste heat is critical. Furthermore, this heat removal must be performed in a manner consistent with maintaining acceptable optical distortions in the laser medium.

One potential IFE concept consists of an end-pumped configuration with the slabs oriented normal to both the pump and extraction beams (see Fig. 1a).[3] The gain medium is segmented into a series of thin slabs, with cooling channels placed between the slabs to accommodate the removal of heat. A high velocity gas flows through the channels to extract the waste heat from the slabs. In rod and single slab geometries (Fig. 1b and 1c), the laser beam never interacts with the cooling fluid. However, in the IFE configuration described in Fig. 1a, the laser extraction beam propagates through both the laser medium and the cooling fluid.

It is precisely this condition, where the laser beam samples both the laser medium and the cooling fluid, that has led to the conjecture that the usefulness of a high average power solid-state device would be severely limited

Sutton

by the effect that variations in heat removal have on laser beam quality. In particular, it has often been assumed that:

(1) the turbulent flow related scattering losses would be unacceptably high.
(2) spatial variations in the cooling rate would result in unacceptably large thermally related optical path length variations in the system.

To address these issues, an experimental facility was developed that allowed detailed investigation of the flow and cooling characteristics of high velocity channel flow.[4,5] Fig. 2 describes the pertinent features of the facility. A single slab was mounted in a central structural assembly, with cooling flow channels formed on both the top and bottom large optical faces. There are three distinct regions to the fixture: nozzle section, entrance region, and heated slab region. Surface heater films were used to simulate the laser slab thermal loading. Fig. 3 describes the flow behavior starting with the end of the nozzle region. At the nozzle exit, the viscous boundary layers are thin compared to the channel thickness. As the flow progresses down the entrance region, the viscous boundary layers grow until they eventually merge at the channel center and the flow becomes fully developed. That is, the velocity profile becomes invariant.

When the flow encounters the heated slab, a thermal boundary layer begins to develop in response to the heating of the flow. It is in this thermal development zone that there can be significant variation in the heat transfer characteristics of the flow. These heat transfer coefficient variations can in turn result in temperature variations in the slab along the flow direction. Additionally, the hot turbulent eddies in the thermal boundary layer are the primary turbulent scattering source.

In the remaining sections of this paper, turbulent scattering losses, heat transfer spatial variations, and thermally induced optical distortions in a single slab are addressed. Experimental results as well as detailed numerical simulations are used to quantify the effects.

2. TURBULENT SCATTERING LOSSES IN HEATED CHANNEL FLOW

As mentioned earlier, one of the primary effects of the cooling flow on optical propagation is the scattering of laser light off hot turbulent eddies. The refractive index fluctuations which cause scattering arise from pressure (cold fluid) and temperature (hot fluid) fluctuations in the turbulent channel flow. When heating of the flow is present, temperature fluctuation effects dominate. For this case, a simple scaling relationship can be developed by noting that the scattering fraction is proportional to the square of the relative density fluctuation ($\Delta\rho/\rho$) which is in turn proportional to the relative temperature fluctuations ($\Delta T/T$).[6] Thus,

$$\frac{I_s}{I_o} \approx \left(\frac{\gamma-1}{\gamma}\right)\left[\left(\frac{G}{a}\right)\left(\frac{q}{M}\right)\right]^2 \qquad (1)$$

where I_o is the incident irradiance, I_s is the scattered irradiance, γ is the ideal gas ratio of specific heats, G is the Gladstone-Dale constant for the gas, a is the gas speed of sound, q is the removed heat flux at the surface, and M is the flow Mach number. The Gladstone-Dale constant relates the index of refraction to density changes through $n-1=G(\rho/\rho_o)$, where n is the index of refraction, ρ is the density, and ρ_o is the reference density. Eq. (1) identifies several important scaling features. First, the scatter fraction should vary as M^{-2} and q^2. Additionally, because cooling gas characteristics are contained in the quantity $[(\gamma-1)/\gamma][G/a]^2$ the scattering fraction will be extremely sensitive to the gas chosen for cooling.

Sutton

The scattering in the heated turbulent channel flow was experimentally measured using a modified Schlieren system.[6] Results for a nitrogen flow are given in Figs. 4. In the ordinate title of these figures, the quantity I_Q-I_b is the scattered intensity associated with heating. Fig. 4a shows the quadratic dependence on the Mach number ($1/M^2$) while Fig. 4b shows the expected quadratic dependence on heat flux. It is clear that heating augmented scattering is reduced with increase in Mach number. However, with nitrogen as the cooling fluid, at even moderate heat fluxes (~1 W/cm^2) and large Mach numbers ($1/M^2 < 5$) the scattering losses per channel will be of order 0.5%. This is orders of magnitude larger than could be tolerated in a large laser system. However, consider the effects of fluid change. For instance, the Gladstone-Dale constant for helium is a factor of 8 smaller than that of nitrogen. Furthermore, the sound speed of helium is a factor of 3 larger. These effects serve to make the parameter $[(\gamma-1)/\gamma][G/a]^2$ ~600 times smaller for helium than nitrogen. Thus, for the same heat flux and Mach number, the scattering losses with helium can be expected to be a factor of ~600 less than for nitrogen. Thus, if helium were used as the cooling fluid, turbulent scattering losses will be negligible even at large Mach numbers and large heat fluxes.

3. COOLING CHANNEL FLOW AND HEAT TRANSFER

Critical to establishing the temperature and stress state in the laser slabs, is quantification of the flow and heat transfer properties of the cooling channel flow. Thermally, we can regard the slab as a heated medium that is influenced by boundary conditions provided by the cooling flow. Since the optical distortions in the laser medium are directly related to the temperature uniformity of the slab, they can in turn be related to the cooling rate at the slab surface. Applying Newton's Law of Cooling, the slab surface temperature is given by

$$T = \frac{q}{h} + T_f \qquad (2)$$

where q is the heat flux removed from the surface, h is the local convective heat transfer coefficient, and T_f is the bulk temperature of the cooling fluid. This equation indicates that the slab temperature will depend strongly on both the fluid temperature and the convective heat transfer coefficient.

Of particular importance, is the quantification of variations in the convective heat transfer coefficient (h). This parameter reflects variations in both the viscous and thermal character of the cooling flow, and as such can result in very large, non-linear cooling rate variations that result in optical path length variations that are difficult to externally correct in any optical system. Fig. 5 shows the calculated variation in the heat transfer coefficient over the thermal development region. Note that there is nearly a factor of four variation in the heat transfer coefficient over the first 0.1 m of thermal development. This calculation was performed using the TEXSTAN computer program,[7] for prototypical IFE design conditions (4 atm pressure, 0.7 Mach number, a channel thickness of 3.6 mm, and a surface heat flux of 0.75 W/cm^2).

Referring to Eq. (2), two things influence the inferred slab temperature. First, since the removed heat flux will be nearly constant over the slab face, changes in the convection coefficient can dramatically alter the difference between the slab surface temperature and the cooling fluid temperature. Additionally, as heat is removed from the laser slab, the cooling fluid bulk temperature increases. This not only takes place during the developing portions of the flow, but also throughout those portions of the flow after a fully developed thermal profile has been established. Thus, while we anticipate variations in the slab temperature during thermal development, variations will also take place after the flow is thermally fully developed because of the caloric heating effect. It is important to note that the temperature variation will be linear in the fully-developed region and highly non-linear in the developing region.

Details of thermal development in the channel have been addressed both experimentally and computationally. Results have been previously reported.[4,5] The TEXSTAN computer program was used to calculate the viscous and thermal boundary layer development, and thus the variation of the convective heat transfer coefficient and the bulk fluid temperature, for the experimental geometry depicted in Fig. 2. A comparison of the experimentally measured and numerically calculated surface temperatures are given in Fig. 6. Note the strong variation in the slab surface temperature over the fist 0.1 m of the slab length, and the excellent agreement between the experimentally measured and calculated surface temperatures. These results serve to not only validate the numerical model, but also demonstrate the strong slab temperature variations that can be present during the early stages of thermal development. Note the linear temperature variation after thermal development takes place. This demonstrates the response of the slab to the continued caloric heating of the cooling fluid.

4. LASER SLAB OPTICAL DISTORTIONS

In characterizing the impact that the cooling fluid and cooling conditions have on the optical characteristics of the system, we are primarily concerned with the optical path variations across the aperture that are the result of cooling induced temperature disturbances in the laser medium. When considering optical path variations associated with the laser medium temperature, to first order only the overall optical path variation across the aperture is of consequence. At any given position in the aperture, the optical path length is given by

$$OPL = \int_s n ds \tag{3}$$

where s is the total path length, and n is the local index of refraction which is given by

$$n = n_o + \frac{\partial n}{\partial T}\Delta T + \frac{\partial n}{\partial \sigma}\sigma \tag{4}$$

In Eq. (4), n_o is the reference index of refraction for the medium being transited by the beam, $\partial n/\partial T$ is the variation of the index with temperature, $\partial n/\partial \sigma$ is the variation of the index with stress, and the quantities ΔT and σ denote temperature and stress variations from the initial stress-free thermal state. Note that both $\partial n/\partial \sigma$ and σ are tensor quantities. Since the slab temperature state is equally influenced by the distribution of deposited energy and the thermal boundary conditions applied on the slab faces, of critical importance is proper characterization of the cooling flow.

The phase variations in the laser beam are conveniently represented as local variations in the optical path length (OPL). This is obtained by evaluating Eq. (3) on a single slab, which requires characterization of the temperature and stress distribution in the slab. The optical distortions were calculated using a sequential application of three codes. First, the temperature distribution was evaluated using the TOPAZ3D[8] computer program. The spatial variation of the heat transfer coefficient and the bulk fluid temperature in each cooling channel is utilized as boundary condition information for the TOPAZ3D calculation. Once the temperature distribution is established, the temperature state is then utilized in the NIKE3D[9] computer program to evaluate the displacements and stresses in the slab. For the cases reported in this paper, mechanically free conditions were applied at each face of the slab. Finally, the temperature and stress distributions were then utilized in the OPTICS[10] code to evaluate the optical path length variation across the aperture.

Fig. 7 shows the effect that material properties can have on the thermally induced optical path variation. In this case, calculations were performed for a 2.03 W/cm^3 uniform thermal load in the slab, and for two radically different laser materials: S-FAP (Fig. 7a) and YAG (Fig. 7b). In each case, the total optical path length variation as well as the contributions from temperature, stress, and displacement are given. The thermal and mechanical properties are given in Table 1. Unfortunately, not all of the necessary thermal, mechanical and optical properties have been measured for S-FAP. Thus, a combination of measured values as well as values inferred from what are believed to be similar materials (FAP and Phosphate glass) are reported in Table 1.

The striking distinction between S-FAP and YAG is the observation that in S-FAP, which has a negative $\partial n/\partial T$, the temperature and displacement effects substantially compensate for each other. On the other hand, for YAG, which has a positive $\partial n/\partial T$ there is no such compensating behavior. As a result, the maximum optical path length variation across the aperture is a factor of 4 less in S-FAP than in YAG. This makes a nearly a-thermal material such as S-FAP highly advantageous since the resulting OPL variations are significantly reduced, which makes optical correction more tractable. It is important to note that a larger negative $\partial n/\partial T$ would increase the compensation and further flatten the profile.

Fig. 8 shows the effect of placing an S-FAP laser slab in two portions of the developing cooling flow. In Fig. 8a, the slab has been located in the thermally developing portion of the flow, while in Fig. 8b the slab is placed in the thermally fully developed portion of the flow, which could be achieved by employing conditioning heaters on the channel walls.[4,5] Note that the optical path length variation is further reduced by over a factor of 6. Additionally, it is substantially more linear than in the case where no thermal conditioning is present. In the case of Fig. 8b, where the heat transfer coefficient is constant over the aperture because the slab is in the thermally fully-developed flow, the optical path length variation is a direct reflection of the temperature rise in the cooling fluid due to simple caloric heating. Once again, a larger negative $\partial n/\partial T$ would further flatten the optical path length variation across the aperture. This serves to demonstrate the importance that proper engineering of laser materials can have on the overall optical performance of the system.

5. SUMMARY AND CONCLUSIONS

In this paper, the issues associated with cooling IFE laser slabs has been addressed. In particular, the effects that the cooling flow has on optical losses and optical distortions have been explored. On the basis of the results presented in this paper, the following conclusions are made:

(1) Gas cooling of an IFE slab amplifier is a viable approach. Adequate cooling can be provided for the IFE design heat flux of 0.75 W/cm^2.

(2) Helium must be used as the cooling fluid to ensure that turbulent scattering losses are not a significant contribution to the overall optical loss in the system. If helium is used, it was shown that scattering losses could be maintained at less than 0.01% per channel. On the other hand, for nitrogen the losses were experimentally demonstrated to be as high as 0.5% per channel.

(3) The selection of an optimal laser material is critical in minimizing optical distortions in the system. In particular, a nearly a-thermal material such as S-FAP offers the advantage of having off-setting effects from the displacement and $\partial n/\partial T$ contributions to optical path length variations across the aperture.

(4) Thermal distortions can be significantly reduced if some form of conditioning of the thermal boundary layer takes place upstream of the laser slab. It was shown that even for a thermally well-behaved material such as

S-FAP, the OPL variations could be reduced by over a factor of two. In addition, the remaining OPL variations are much more linear, signifying the necessity for only simple beam steering correction in the system.

6. ACKNOWLEDGMENTS

This work was performed under the auspices of the U.S. Department of Energy by the Lawrence Livermore National Laboratory under Contract W-7405-Eng-48. The authors thank W. Krupke and S. Payne for their continued support of the gas-cooled slab concept, L. DeLoach for measurements of the S-FAP properties, and C. Marshall for numerous useful discussions. The authors gratefully acknowledge the contributions of H. F. Robey, B. L. Freitas, and A. Erlandson to some aspects of the experimental effort, and M. Crawford of the University of Texas for the use of the TEXSTAN computer program.

7. REFERENCES

1. L. D. DeLoach, S. A. Payne, L, K. Smith, W. L Kway, and W. F. Krupke, "Laser and Spectroscopic Properties of $Sr_5(PO_4)_3F$:YB," J. Opt. Soc. Am. B, Vol. 11, No. 2, pp. 269, 1994.

2. R. Beach, W. Benett, B. Freitas, D. Mundinger, B. Comaskey, R. Solarz, M. Emanuel, "Modular Microchannel Cooled Heatsinks for High Average Power Laser Diode Arrays," IEEE J. Quantum Electron., Vol. 28, No. 4, pp. 966, 1992.

3. C. D. Orth, S. A. Payne, and W. F. Krupke, "A Diode-Pumped Solid-State Laser Driver for Inertial Fusion Energy," accepted for publication in Nuclear Fusion.

4. S. B. Sutton, G. F. Albrecht, and H. F. Robey, "Heat Removal in a Gas Cooled Solid-State Laser Disk Amplifier," J. AIAA, Vol. 30, No. 2, pp. 431-435, February 1992.

5. S. B. Sutton, G. F. Albrecht, H. F. Robey, and B. L. Freitas, "Thermal Management in Gas Cooled Solid-State Laser Disk Amplifiers," AIAA 23rd Plasmadynamics and Lasers Conference, July 6-8, 1992.

6. G. F. Albrecht, H. F. Robey, and A. C. Erlandson, "Optical properties of turbulent channel flow," Applied Optics, Vol. 29, No. 21, pp. 3079-3087, July 1990.

7. TEXSTAN is a variation, written by M.E. Crawford of the University of Texas, of the STAN5 computer program: M. E. Crawford and W. M. Kays, "STAN5 - A Program for Numerical Computation of Two-dimensional Internal and External Boundary Layer Flow," NASA Report No. CR-2742, November 1976.

8. A. Shapriro, "TOPAZ3D - A Three-Dimensional Finite Element Heat Transfer Code," Lawrence Livermore National Laboratory, UCID-20484, 1985.

9. B. N. Maker, R. M. Ferencz, and J. O. Hallquist, "NIKE3D - A Nonlinear, Implicit, Three-Dimensional Finite Element Code for Solid and Structural Mechanics," Lawrence Livermore National Laboratory, UCRL-MA-105268, January 1991.

10. The optics code applied in these calculations is an adaptation of: S. K. Doss, "Physics and Mathematics of the BREW Code," *1986 Laser Program Annual Report*, Lawrence Livermore National Laboratory, UCRL-50021-86, pp. 7-132 - 7-135, November 1987.

Sutton

Table 1

Material Properties

Property	S-FAP	YAG
Thermal conductivity (W/m-K)	2.0 [(a)]	9.8
Young's modulus (GPa)	119 [(a)]	280
Poisson's ratio	0.26 [(a)]	0.28
Thermal expansion coefficient (K^{-1})	$1.e^{-5}$ [(a)]	$6.7x10^{-6}$
Index of refraction	1.628 [(b)]	1.816
$\partial n/\partial T$ (K^{-1})	$-5.0x10^{-6}$ [(b)]	$9.86x10^{-6}$
Piezo-Optic coefficients:		
π_{11} (Pa^{-1})	$9.36x10^{-13}$ [(c)]	$-1.209x10^{-13}$
π_{12} (Pa^{-1})	$1.86x10^{-12}$ [(c)]	$5.203x10^{-14}$
π_{44} (Pa^{-1})		$-5.583x10^{-13}$

(a) FAP property
(b) Measured S-FAP property
(c) Measured Phosphate glass property

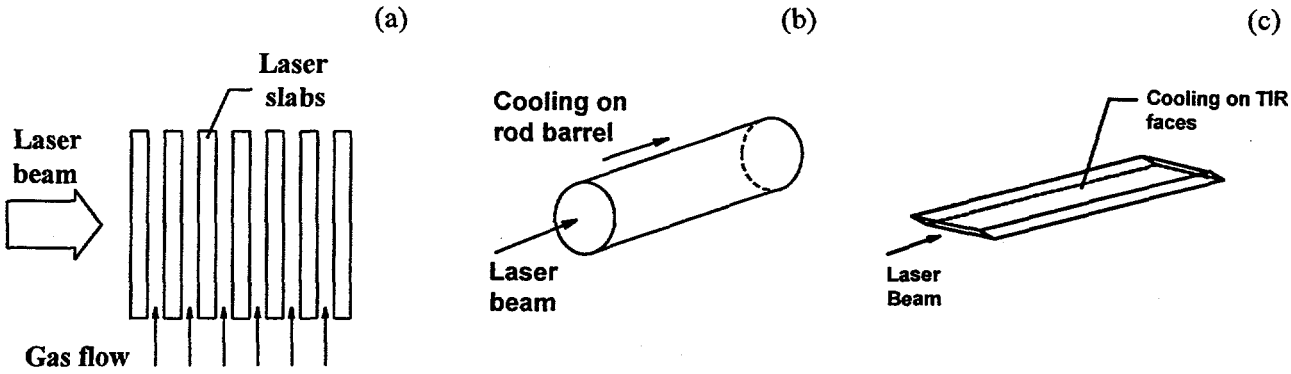

Fig. 1 - In the IFE laser concept, the impact of the cooling flow on laser propagation is much different than in other laser architectures. In rod (b) and single slab (c) architectures, the laser beam never samples the cooling fluid. In the IFE architecture (a), where cooling takes place from the large optical surfaces, the laser beam samples each of the cooling channels.

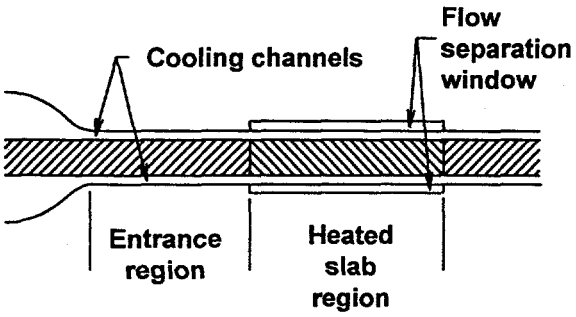

Fig. 2 - The geometry of the flow fixture, which consisted of a single slab surrounded by two flow channels. The fixture included an entrance region where the viscous boundary layers were established and the heated slab region, where resistive film heaters were used to simulate the thermal loading in the slab.

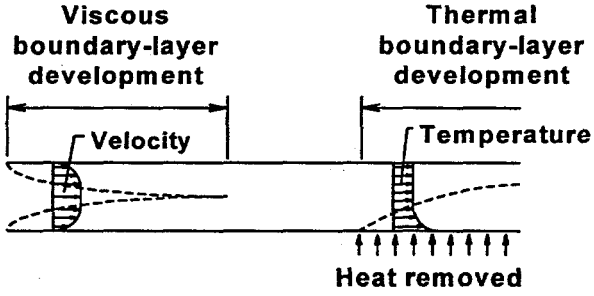

Fig. 3 - A depiction of the two boundary layer development regions in the channel flow: (1) the viscous entry region where the velocity distribution is established, and (2) the thermal development region that starts at the first point where heating of the flow occurs

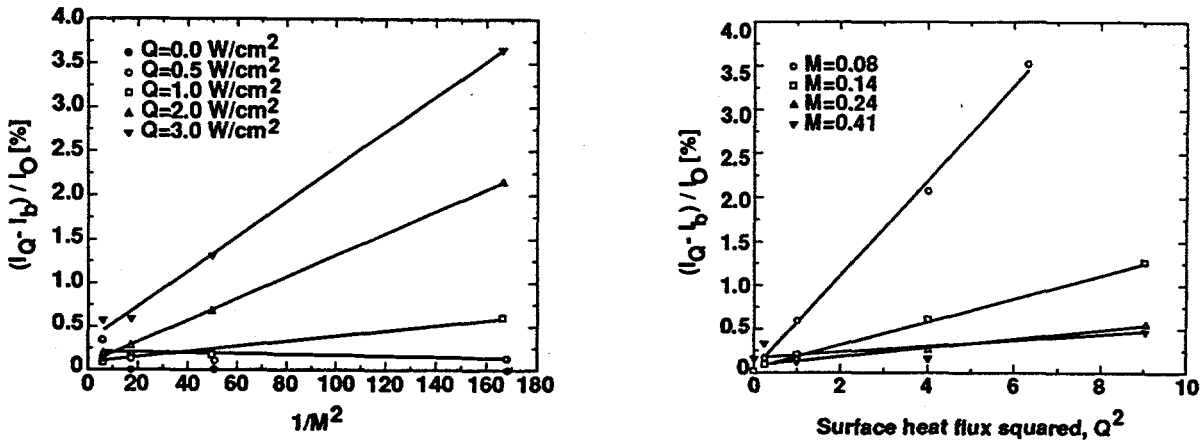

Fig. 4 - Experimental verification of the quadratic dependence of the scattered fraction on the heat flux and the flow Mach number. (a) the scattered fraction as a function of the inverse square of the Mach number, (b) the scattered fraction as a function of the square of the heat flux

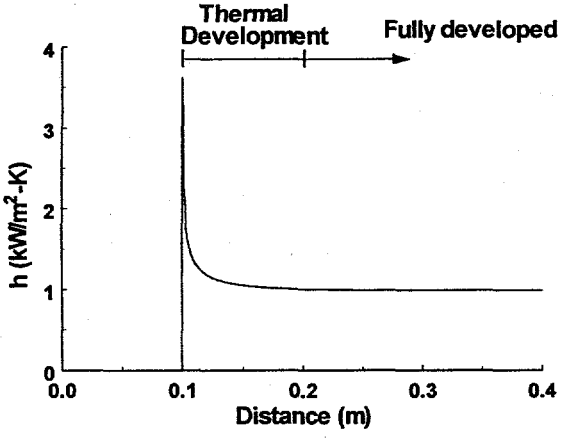

Fig. 5 - The calculated variation of the heat transfer coefficient during the development of the thermal boundary layer. This calculation was for prototypical IFE flow conditions of 4 atm. pressure, 0.7 Mach number flow, 3.6 mm channel thickness, and a surface heat flux of 0.75 /.cm^2.

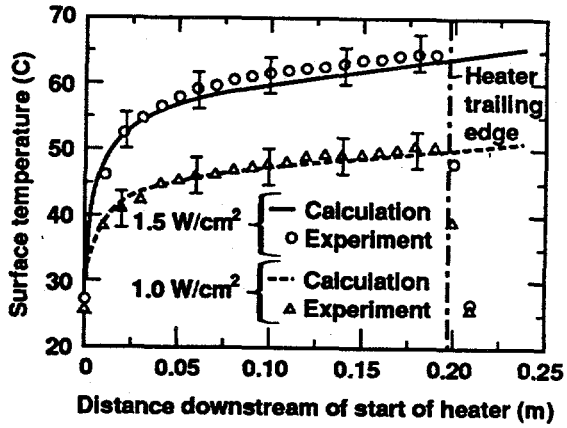

Fig. 6 - Surface temperature variation over the heated slab without upstream thermal conditioning. Experiments and calculations are compared for heat flux values of 1 and 1.5 W/cm^2 in 2.06 atm., Mach 0.13 nitrogen flow

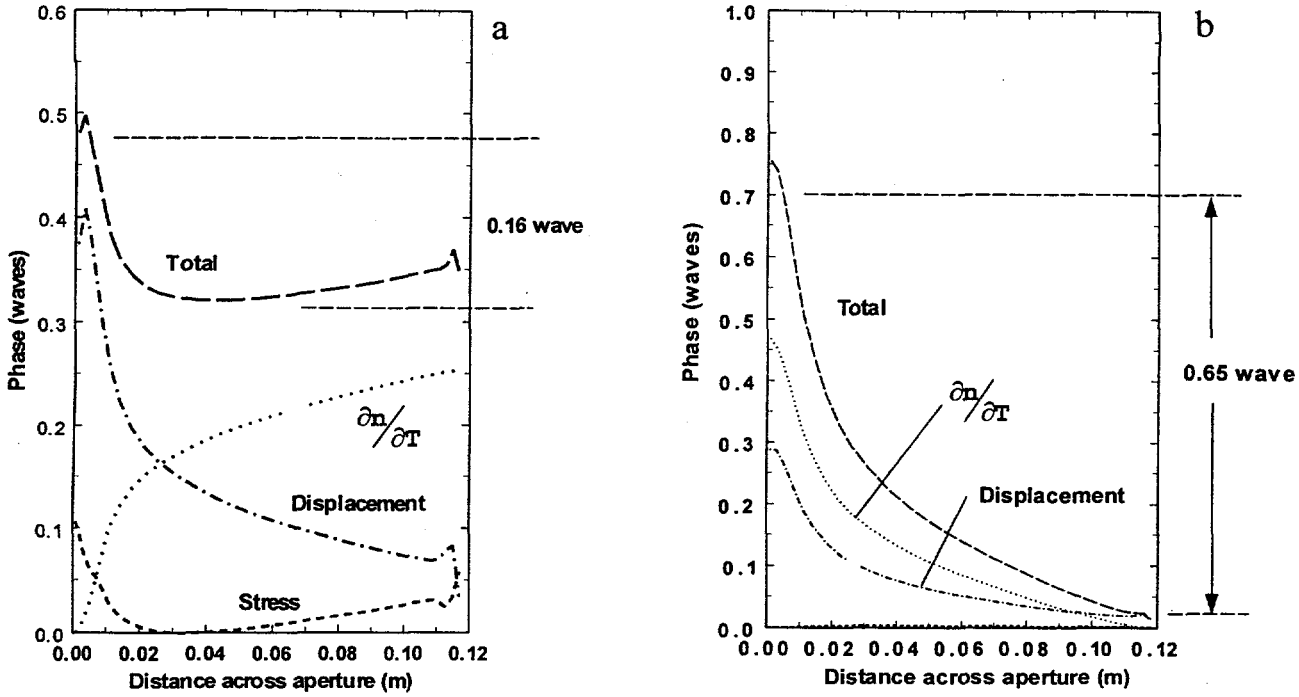

Fig. 7 The effect of material properties on optical path length variations. (a) S-FAP without thermal conditioning. (b) YAG without thermal conditioning.

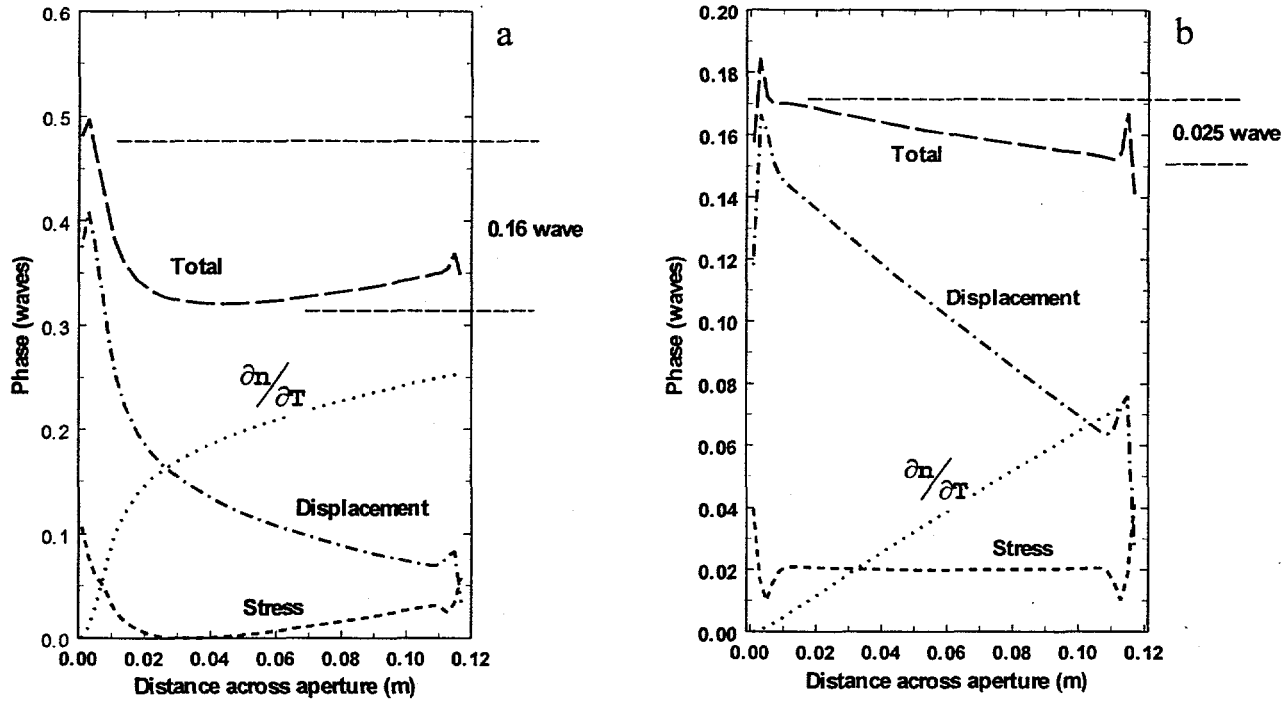

Fig. 8 - The effect of thermally conditioning the cooling flow. (a) S-FAP without thermal conditioning, (b) S-FAP with thermal conditioning.

Sutton